analytical chemistry

Article

pubs.acs.org/ac

Application of a High-Resolution Mass-Spectrometry-Based DNA Adductomics Approach for Identification of DNA Adducts in Complex Mixtures

Silvia Balbo,* Stephen S. Hecht, Pramod Upadhyaya, and Peter W. Villalta

Masonic Cancer Center, University of Minnesota, 2231 6th Street SE, Minneapolis, MN 55455

ABSTRACT: Liquid chromatography coupled with mass spectrometry (LC-MS) is the method of choice for analysis of covalent modification of DNA. DNA adductomics is an extension of this approach allowing for the screening for both known and unknown DNA adducts. In the research reported here, a new high-resolution/accurate mass MS^n methodology has been developed representing an important advance for the investigation of in vivo biological samples and for the assessment of DNA damage from various human exposures. The methodology was tested and optimized using a mixture of 18 DNA adducts representing a range of biologically relevant modifications on all four bases and using DNA from liver tissue of mice exposed to the tobacco-specific nitrosamine 4-(methylnitrosamino)-1-(3-pyridyl)-1-butanone (NNK). In the latter experiment, previously characterized adducts, both expected and unexpected, were observed.

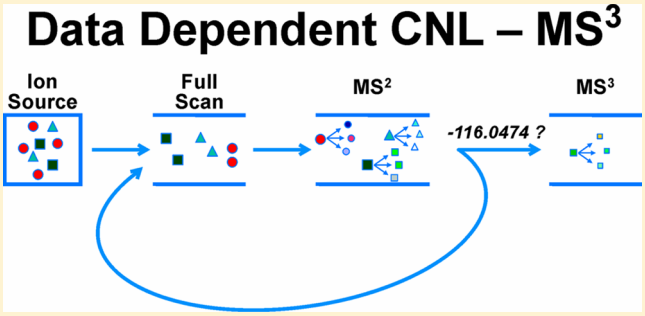

Liquid chromatography coupled with mass spectrometry (LC-MS) has become the method of choice for the characterization and quantitation of covalent modification of DNA in various biological samples.[1,2] However, the standard methodology focuses on the investigation of small numbers of anticipated DNA adducts based on a priori assumptions regarding the formation of specific adducts. This approach does not account for the complexity of in vivo DNA adduct formation resulting from endogenous sources, such as oxidative stress or lipid peroxidation, or as a result of exposure to complex mixtures of chemicals which cannot be completely anticipated or predicted. In the era of genome-wide association studies and development of -omics techniques, new technologies are needed to allow investigation of effects arising from environmental exposure in all its complexity.[3] In this context, DNA adductomics is emerging as a method for screening for both known and unknown DNA adducts and is prompting activity by several research groups.[4−15]

The LC-MS^n methodology for adductomics experiments relies primarily on the general observation that the collisional-induced dissociation of protonated modified deoxyribonucleoside ions results in the loss of the deoxyribose moiety and the formation of the corresponding protonated modified nucleobase ions. In a typical experiment, DNA samples are enzymatically hydrolyzed to free deoxyribonucleosides with the resulting sample analyzed by LC-MS^n for neutral loss of m/z = 116 corresponding to the deoxyribose group.

The most common approach has been to perform LC-MS^2 analysis using triple quadrupole instrumentation operated in the constant neutral loss (CNL)[6−8,13] or "pseudo" CNL mode.[5,9−12,14] In CNL mode, quadrupole 1 (Q1) and Q3 are scanned simultaneously over a large mass range with a constant offset of 116 amu. The pseudo-CNL approach is similar to CNL; however, instead of actually scanning the quadrupoles, the system is set to monitor many (25 to 50) 1 amu spaced contiguous selected reaction monitoring (SRM) transitions all involving the loss of 116 amu with multiple injections (typically 7−15) covering different mass ranges, so that a large range is ultimately covered for a given sample. The triple quadrupole approach has many positive attributes including simplicity of both methodology and data analysis and relatively low instrumentation costs. However, it is limited in both its selectivity and identification capability due to its "low-resolution" data acquisition and lack of fragmentation beyond MS^2.

The field of DNA adductomics is in its infancy, and thus there are many opportunities for significant improvement, especially considering the rapidly improving capabilities of MS instrumentation. The method we describe here is a unique and innovative nanoelectrospray ionization/high-resolution MS approach. It uses high-resolution/accurate mass monitoring of the neutral loss of the 2′-deoxyribose (116.0474 amu) moiety with triggering of MS^3 fragmentation to increase the specificity of the fundamental adduct identification step and the presence of an MS^3 event indicating the observation of an adduct. In addition, the accurate mass measurement of the observed DNA adducts allows for determination of the likely elemental composition of the adduct. The MS^3 fragmentation which is

Received: November 4, 2013
Accepted: January 10, 2014
Published: January 10, 2014

   dx.doi.org/10.1021/ac403565m | *Anal. Chem.* 2014, 86, 1744−1752

triggered upon observation of the accurate mass loss of deoxyribose provides additional adduct structural information. Finally, the methodology outlined here is unique in that it uses nanospray ionization (300 nL/min) to take advantage of the inverse relationship between flow rate and electrospray sensitivity.[16,17] This maximized sensitivity is especially important, because sample sizes of in vivo sources of DNA are typically limited and adduct levels are low.

In the research reported here, we tested and optimized the performance of the approach by analyzing a mixture of 18 DNA adducts including modifications of all four nucleobases at various reactive sites producing adducts with differing polarities. We also investigated the effect of a real sample matrix on DNA adduct detection in the standard mix. Lastly, DNA from liver tissue of mice exposed to the tobacco-specific nitrosamine 4-(methylnitrosamino)-1-(3-pyridyl)-1-butanone (NNK) was analyzed to assess the ability of the method to detect expected DNA adducts and screen for unknown adducts formed in vivo.

EXPERIMENTAL SECTION

Caution. NNK is carcinogenic. It should be handled with extreme caution in a well-ventilated hood and with personal protective equipment.

Chemicals. N^2-ethyl-2′-deoxyguanosine (N^2-ethyl-dG) (**1**), N^2-(4-hydroxybut-1-yl)deoxyguanosine [N^2-(4-OH-butyl)-dG] (**2**), (6*S*,8*S*)-3-(2′-deoxyribos-1′-yl)-5,6,7,8-tetrahydro-8-hydroxy-6-methylpyrimido[1,2-a]purine-10(3*H*)one (OH−Methyl-PdG) (**3**), (6*R*/*S*)-3-(2′-deoxyribos-1′-yl)-5,6,7,8-tetrahydro-6-hydroxypyrimido[1,2-a]-purine-10(3*H*)one (OH-PdG) (**4**), 7,8,9-trihydroxy-10-(N^2-deoxyguanosyl)-7,8,9,10-tetrahydrobenzo[a]pyrene (BPDE N^2-dG) (**5**), 5-methylchrysene-diolepoxide-N^2-deoxyguanosine ((5-MeCDE-N^2-dG) (**6**), O^6-[4-(3-pyridyl)-4-oxobut-1-yl]-2′-deoxyguanosine (O^6-POB-dG) (**9**), O^6-[1-hydroxy-1-(3-pyridyl)but-4-yl]deoxyguanosine (O^6-PHB-dG) (**10**), 5-methylchrysene-diolepoxide- N^6-deoxyadenosine (5-MeCDE-N^6-dA) (**14**), O^4-(4-hydroxybut-1-yl)-thymidine [O^4-(4-OH-butyl)-dT] (**15**), O^2-[4-(3-pyridyl)-4-oxobut-1-yl]thymidine (O^2-POB-dT) (**16**), N^4-(4-hydroxybut-1-yl)deoxycytidine [N^4-(4-OH-butyl)-dC] (**17**) and O^2[4-(3-pyridyl)-4-oxobut-1-yl]deoxycytidine (O^2-POB-dC) (**18**), were prepared as described.[18−24] O^6-Methyl-2′-deoxyguanosine (O^6-Me-dG) (**7**), 8-oxo-7,8-dihydro-2′-deoxyguanosine (8-Oxo-dG) (**8**), 1,N^6-etheno-2′-deoxyadenosine (ε-dA) (**12**) and N^6-hydroxymethyldeoxyadenosine (N^6-Me-dA) (**13**) were purchased from Sigma-Aldrich (St. Louis, MO). 6-(1-Hydroxyhexanyl)-8-hydroxy-1,N^2-propano-2-deoxyguansine (HNE-dG) (**11**) was kindly donated by Dr Fung-Lung Chung from Georgetown University Medical Center. The mixture of 18 standards was dissolved in H_2O/CH_3OH 80:20 at a final concentration of 100 fmol/μL for each standard. Ethanol was obtained from AAPER Alcohol and Chemical Co. (Shelbyville, KY). Puregene DNA purification solutions were obtained from Qiagen (Valencia, CA). Calf thymus DNA was purchased from Worthington Biochemical Corporation (Lakewood, NJ). All other chemicals were purchased from Sigma-Aldrich. All solvents used for HPLC and MS analysis were of the purest grade commercially available.

Human Leukocyte DNA. This study was approved by the University of Minnesota Institutional Review Board. Blood samples were obtained by venipuncture from two nonsmokers. Leukocytes were isolated from freshly collected peripheral whole blood. DNA was isolated using the DNA purification from the buffy coat protocol (Qiagen Corp, Valencia, CA) with several modifications.[25] Briefly, 3 mL of RBC cell lysis solution were added to 1 mL of buffy coat prepared from 10 mL of whole blood. The white blood cell pellet was collected by centrifugation (2000*g* × 10 min), treated with 3 mL of cell lysis solution and incubated at room temperature overnight. A solution of RNase A (4 mg/mL) was added (15 μL), and the sample was incubated at room temperature for 2 h. One milliliter of protein precipitation solution was added to the cell lysate, and the mixture was centrifuged (2000*g* × 15 min) to remove proteins. DNA was precipitated from the supernatant by addition of 4 mL of isopropanol. The DNA pellet was washed with 1 mL of 70% ethanol in H_2O and then 1 mL of 100% ethanol. DNA was dried in a stream of N_2 and stored at −20 °C until use.

Treatment of Mice with NNK. This study was approved by the University of Minnesota Institutional Animal Care and Use Committee and was performed in accordance with NIH guidelines. Female A/J mice, 5−6 weeks old, were purchased from Jackson Laboratories (Bar Harbor, ME) and were housed, five animals per cage, under standard conditions and maintained on American Institute of Nutrition-93-G diet (Dyets, Inc., Bethlehem, PA). Animals were exposed to 3 μmol (621 μg) NNK, by gavage in 0.1 mL of cotton seed oil once a week for 4 weeks, and were sacrificed 24 h after the last treatment. Livers were removed, immediately frozen on dry ice, and stored at −80 °C.

DNA Isolation from Mouse Liver. Mouse liver (700 mg) was cut into small pieces, added to 12 mL cell lysis solution (Qiagen), and homogenized with a Tissue Ruptor (Qiagen) for 2 min at medium speed. The sample was then processed as reported above following the protocol for DNA isolation from human leukocytes. Reagent volumes were scaled accordingly following the manufacturer's recommendations.

DNA Hydrolysis. DNA (~500 μg) was dissolved in 400 μL 10 mM Tris/5 mM $MgCl_2$ buffer (pH 7) and was initially digested overnight at room temperature with 350 units (U) of DNase I (type II, from bovine pancreas). To the resulting mixture were added an additional 350 additional U of DNase I, 225 mU of phosphodiesterase I, 32.5 mU of phosphodiesterase II, and 750 U of alkaline phosphatase, followed by incubation at 37 °C overnight. The enzymes were then removed by centrifugation using a centrifree MPS ultrafiltration device (MW cutoff of 30 000; Amicon, Beverly, MA). All steps of the protocol were performed using silanized glass vials.

HPLC Purification and Fraction Collection. The hydrolysate was reduced to a volume of about 300 μL under reduced pressure. Fractionation was carried out with an Agilent 1100 HPLC with a diode array UV detector operated at 254 nm (Agilent Technologies, Palo Alto, CA). A 4.6 × 25 cm Luna 5 μm C18 column (Phenomenex, Torrance, CA) was used with a CH_3OH in H_2O gradient at a flow rate of 700 μL/min. The gradient was as follows: 5% CH_3OH, 5 min; then increased to 20% CH_3OH in 1 min and held for 5 min; then increased to 30% in 2 min and held for 5 min; then to 40% in 1 min and held for 5 min; then to 50% in 1 min and held for 5 min; then to 70% in 1 min and held for 5 min; and finally to 100% in 1 min and held for 5 min between 37 and 43 min. Fraction collection started 6 min after the beginning of the run. Fractions were collected every 3 min for a total of 12 fractions collected for each sample injected. The fractions were then dried under reduced pressure. Residuals from fractions 2 to 7 were resuspended in 20 μL H_2O, whereas residuals from fractions 8 to 12 were resuspended in 20 μL of 20% CH_3OH in

dx.doi.org/10.1021/ac403565m | Anal. Chem. 2014, 86, 1744−1752

H_2O. All steps of the protocol were performed using silanized glass vials.

LC-MS Parameters. One microliter of sample was injected onto a NanoLC-Ultra 2D HPLC (Eksigent, Dublin, CA) system equipped with a 5 μL injection loop. Separation was performed with a capillary column (75 μm ID, 10 cm length, 15 μm orifice) created by hand packing a commercially available fused-silica emitter (New Objective, Woburn MA) with 5 μm Luna C18 bonded separation media (Phenomenex, Torrance, CA). The flow rate was 1000 nL/min for 5.5 min, then decreased to 300 nL/min with a 40 min linear gradient of 2 to 30% CH_3CN in 5 mM NH_4OAc aqueous buffer (pH 6.8), followed by a 5:95 buffer/CH_3CN hold for 10 min and a 5 min re-equilibration at 1000 nL/min 98:2 buffer/CH_3CN. The injection valve was switched at 6 min to remove the sample loop from the flow path during the gradient. Samples were analyzed by nanoelectrospray using an LTQ Orbitrap Velos instrument (Thermo Scientific, Waltham, MA). The nanoelectrospray source voltage was set at 1.6 kV, and the capillary temperature was 350 °C. The ion focusing and transfer elements of the instrument were adjusted for maximum signal intensity by using the automated instrument tuning feature while monitoring the background ion signal of m/z = 371.1 amu (decamethylcyclopentasiloxane) to create the tune file used for data analysis. This resulted in an S-Lens RF level setting of 62%.

CNL-MS^n Data-Dependent Scanning. Analysis was performed with full scan detection followed by data-dependent MS^2 acquisition and constant neutral loss triggering of MS^3 fragmentation. Full scan (250−600 amu) detection was performed using the Orbitrap detector at a resolution of 60 000 (at m/z 400) with 1 microscan (one mass analysis followed by ion detection), automatic gain control (AGC) target settings of 1×10^6, and a maximum ion injection time setting of 100 ms. For the analysis of mouse liver DNA, seven injections were made using different 50 amu ranges covering a total range of 250−600 amu. MS^2 fragmentation was performed in the ion trap on the three most intense full scan ions from the full scan spectra with Orbitrap detection at a resolution of 7500, automatic gain control (AGC) of 2×10^5, 1 microscan, maximum ion injection time of 100 ms, and full scan injection waveforms enabled. MS^2 fragmentation parameters were as follows: 3 amu isolation width, normalized collision energy of 35, activation Q of 0.25, and activation time of 10 ms. Data-dependent parameters were as follows: triggering threshold of 500, repeat count of 1, exclusion list size of 500, exclusion duration of 60s, and exclusion mass width of ±5 ppm. A reject mass list (500 ions) was used with a mass tolerance of ±5 ppm consisting of protonated 2′-deoxyribonucleosides and protonated 2′-deoxyribonucleoside artifacts as listed in Table 1 and the most intense peaks observed in the full scan (250−600 amu) mass analysis over the total chromatographic time period of a sample preparation blank. MS^3 fragmentation (2 amu isolation width, normalized collision energy of 35, activation Q of 0.25, activation time of 30 ms) with ion trap detection was triggered upon observation of a neutral loss of 116.0474 ± 0.0006 amu (±5 ppm) between the parent ion and one of the 50 most intense product ions from the MS^2 spectrum, provided a minimum signal of 500 was observed. The following MS^3 parameters were used: 3 microscans, repeat count of 1, AGC target setting 1×10^4, maximum ion injection time of 50 ms.

Table 1. List of the Calculated Masses (m/z) of Positively Ionized 2′-Deoxyribonucleoside Ions for the Four Bases and Their Corresponding Electrostatically Bound Dimer Ions

	$+H^+$	$+K^+$	$+Na^+$	$+NH_3^+$
dG	268.1040	306.0599	290.0860	285.1306
dA	252.1091	290.0650	274.0911	269.1357
dC	228.0979	266.0538	250.0798	245.1244
dT	243.0975	281.0534	265.0795	260.1241
dGdG	535.2008	573.1567	557.1827	552.2273
dGdA	519.2059	557.1617	541.1878	536.2324
dGdC	495.1946	533.1505	517.1766	512.2212
dGdT	510.1943	548.1502	532.1762	527.2208
dAdA	503.2110	541.1668	525.1929	520.2375
dAdC	479.1997	517.1556	501.1817	496.2263
dAdT	494.1994	532.1553	516.1813	511.2259
dCdC	455.1885	493.1444	477.1704	472.2150
dCdT	470.1881	508.1440	492.1701	487.2147
dTdT	485.1878	523.1437	507.1698	502.2144

RESULTS AND DISCUSSION

We used a mixture of 18 DNA adduct standards (Figure 1) to test and optimize our methodology. The selected adducts represent modifications of all four nucleobases at various reactive sites and with differing polarity. The standards were dissolved in H_2O or CH_3OH, combined, and diluted with H_2O to reach a final concentration of 100 fmol/μL. One microliter injections were made. The instrument was set to perform three scan events: (1) full scan from m/z 250 to 600 at a resolution of 60 000; (2) data-dependent MS^2 analysis (R = 7500) of ions observed in the full scan event; (3) data-dependent MS^3 analysis triggered by the neutral loss of 116.0474 ± 0.0006 amu from the MS^2 spectrum and the mass of the ion which triggered the MS^2 event.

The high-resolution/accurate mass measurements of the parent and product ions allow for selective identification of DNA adducts with minimal possibility of false positives while providing valuable molecular formula information. In addition, data-dependent operation is efficient, because ions can be selected (and rejected) for MS^2 fragmentation based upon their accurate masses. Also, it allows for a higher number (50) of product ions considered for MS^3 fragmentation compared to the similar "low-resolution" ion trap methodology of Turesky et al.,[4] which used a value of 10.

Preliminary data from the analysis of DNA samples using the methodology described here suggested that the limiting factor for low level adduct detection was the speed at which ions could be sampled for MS^2 fragmentation. To maximize the sampling rate, one microscan was used for the full and MS^2 scan events with a repeat count value of one for MS^2 and MS^3 scan events. Increasing the number of microscans should result in more sensitive detection of adducts, and higher numbers of repeat counts and microscans would result in higher certainty of MS^2 loss of the ribose moiety (116.0474 amu) and higher quality MS^2 and MS^3 spectra. Initial tests suggested that a repeat count of 1 was sufficient for the MS^2 identification of DNA adducts and MS^3 spectra which matched those of synthetic standards. Increasing the repeat count for the MS^3 scan events could be done with minimal impact on the overall sampling rate, because the majority of the instrument time is spent on the full scan and MS^2 scan events. A relatively high-resolution setting of 60 000 was used for full scan analysis to differentiate the complex set of ions observed. A significantly

dx.doi.org/10.1021/ac403565m | Anal. Chem. 2014, 86, 1744−1752

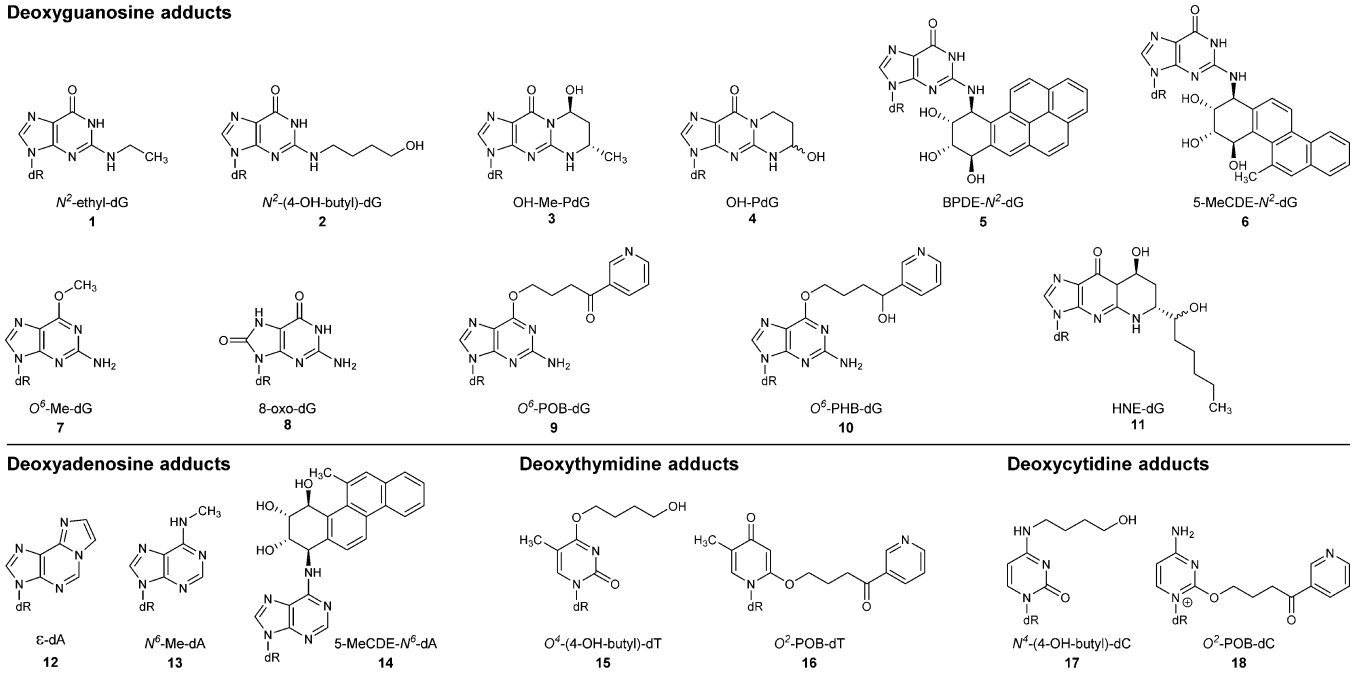

Figure 1. Structures of the DNA adducts in the mixture of standards, dR = 2′-deoxyribose.

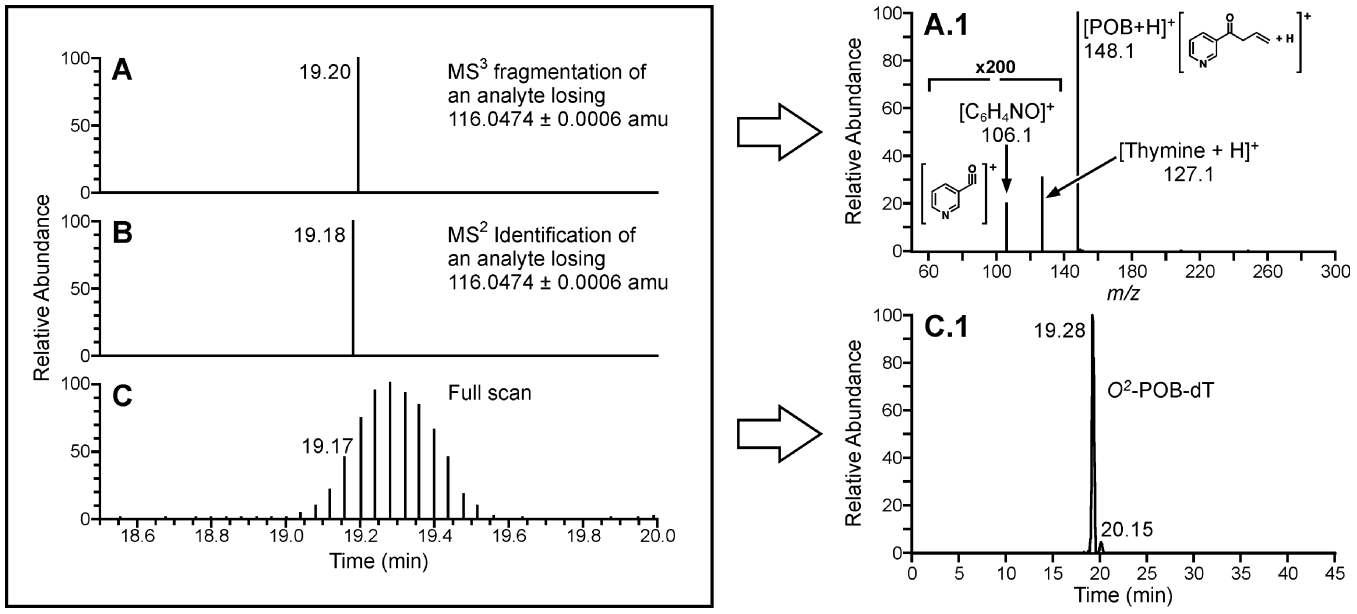

Figure 2. Output of the high-resolution/accurate mass adductomic approach illustrated in the chromatograms and spectrum shown for O^2-POB-dT from the standard mixture analysis. Panel A shows the MS^3 scan event signifying detection of an adduct triggered by a mass difference of 116.0474 amu between an ion mass in the full scan (event shown in Panel C at 19.17 min) and an ion mass in the corresponding triggered MS^2 spectrum (event shown in Panel B). Panel A.1 is the MS^3 spectrum of O^2-POB-dT. Panel C.1 is the accurate mass (5 ppm) extracted ion chromatogram of m/z = 390.1660 amu (O^2-POB-dT) from the full scan spectra..

lower resolution of 7500 was used for the MS^2 analysis, because the fragmentation spectra is much less complex and scanning time of an Orbitrap analyzer is inversely proportional to resolution. The lower resolution setting of the MS^2 spectra does not affect the ability of the Orbitrap to make accurate mass measurements unless there are no unresolved fragment ions skewing the measured nucleoside ion mass from the true value. Three microscans were used for the MS^3 events to increase the amount of ion signal detected (compared to one microscan for MS^2 events) with little impact on the MS^2 sampling rate, because the number of MS^3 triggered events is relatively small.

An example of the set of data obtained from each adduct identification is shown for O^2-POB-dT in Figure 2. The signal generated by the MS^3 fragmentation event as shown in Panel A indicates the observance of a DNA adduct with the corresponding MS^3 spectrum providing structural information including possible base identification. In this example, the MS^3 spectrum of O^2-POB-dT (shown in Panel A.1) contains $[POB]^+$ (m/z = 148.1 amu), $[thymine + H]^+$ (m/z = 127.1

dx.doi.org/10.1021/ac403565m | Anal. Chem. 2014, 86, 1744−1752

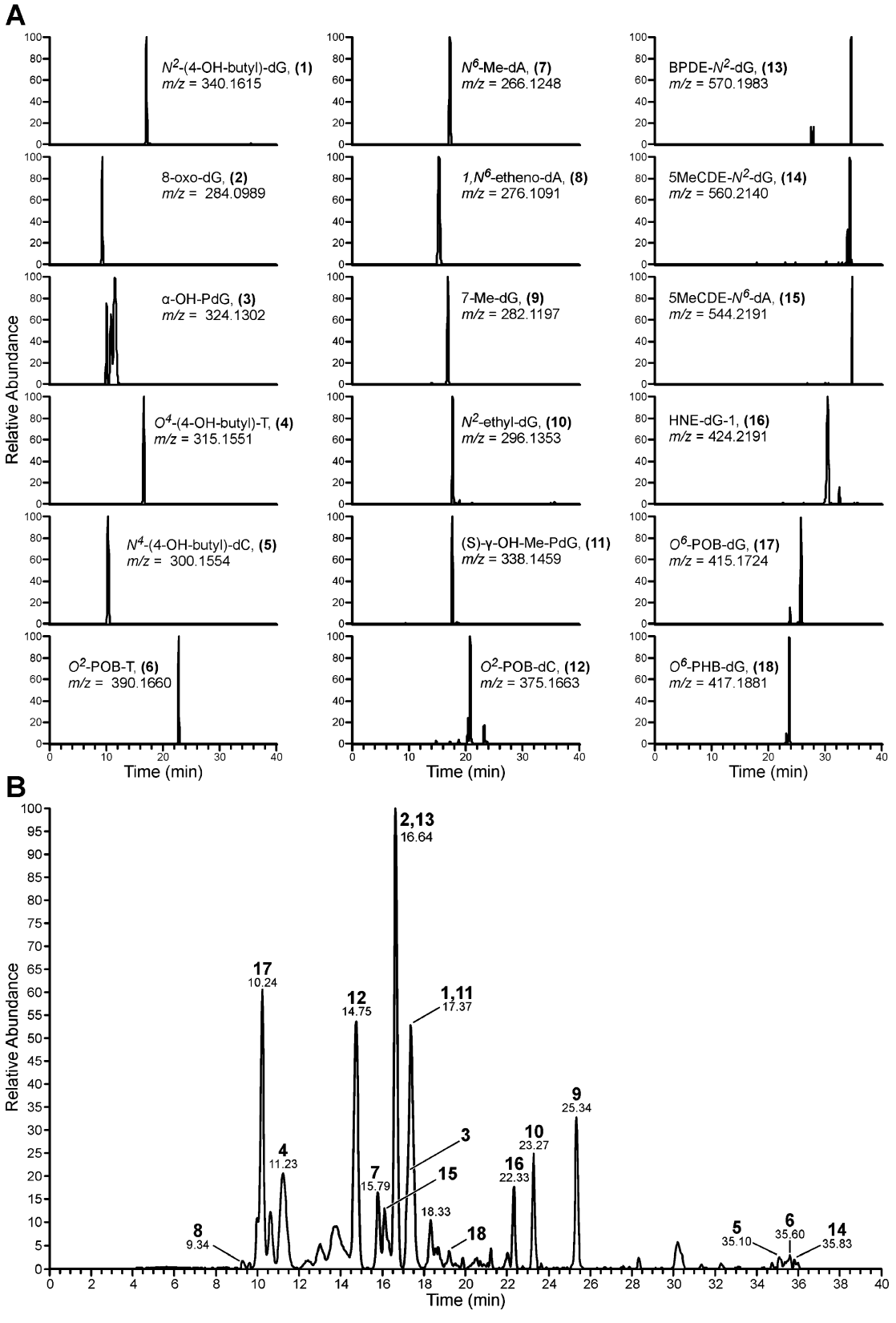

Figure 3. Chromatograms obtained upon analysis of a mixture of 18 DNA adducts (20 fmol of each). Panel A: each channel shows the full scan accurate mass extracted ion chromatogram of the DNA adducts. Panel B: chromatogram combining the extracted ion chromatograms of all 18 adducts.

amu), and $[C_6H_4NO]^+$ (m/z = 106.1 amu) as fragment ions of $[O^2$-POB-dT + H − 116.0474$]^+$. The measured accurate mass of O^2-POB-T is determined from the ion mass in the MS^2 spectrum which triggered the MS^3 event. Likewise, the measured mass of O^2-POB-dT is determined from the full scan ion which triggered the MS^2 event (shown in Panel B).

dx.doi.org/10.1021/ac403565m | Anal. Chem. 2014, 86, 1744−1752

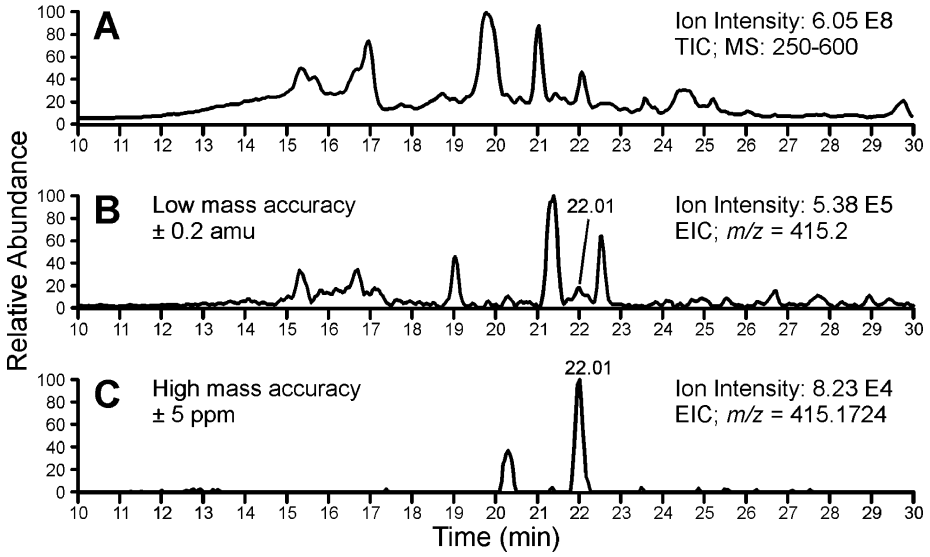

Figure 4. Chromatograms obtained upon analysis of an HPLC fraction (fraction 9) from a human leukocyte DNA sample spiked with the mix of 18 standards. Panel A: total ion chromatogram (TIC) of the full scan data (250−600 amu) with high background signal from the sample matrix, which does not allow for clear identification of any peak. Panel B: extracted ion chromatogram (EIC) for O^6-POB-dG at a mass tolerance typical of quadrupole and ion trap instruments (±0.2 amu). The peak corresponding to O^6-POB-dG is not clearly distinguishable. Panel C: extracted ion chromatogram (EIC) for O^6-POB-dG at a mass tolerance of 5 ppm. The DNA adduct peak is clearly identifiable.

Because the data-dependent repeat count was set to one for both the MS^2 and MS^3 scan events, there is one MS^2 spectrum and one MS^3 spectrum acquired for O^2-POB-dT. The measured mass of O^2-POB-dT, as determined from the full scan spectrum corresponding to the event at 19.17 min, represented in Panel C, is 390.1658 amu, which is 0.5 ppm from the actual mass (390.1660 amu).

Accurate mass extracted ion chromatograms for all standards showed clear and sharp peaks as illustrated in Figure 3. All standards triggered MS^2 fragmentation resulting in the loss of deoxyribose (116.0474 ± 0.0006 amu) at high mass tolerance with subsequent triggering of the MS^3 events.

Fragmentation parameters were optimized using the 18 adduct mix. The CID collision energy, isolation width, activation time, and activation Q were varied while monitoring the number of MS^3-triggered events and the MS^2 signal intensity. Variation of the activation time and activation Q from the instrument default values had no effect on signal intensity. No differences were observed when varying the CID collision energy from 25 to 55. The isolation width optimization was more complicated. MS^2 signal intensity increased and reached a plateau as the isolation window was increased and the onset value of the plateau increased with increasing ion mass. As a compromise between sensitivity and selectivity, the onset value for a DNA adduct [N^2-(4-OH-butyl)-dG] which had an intermediate mass (m/z = 340 amu) was determined to be 3 amu and was used in the method. The number of ions fragmented per full scan was varied, and the optimal value in terms of triggering of MS^3 events was determined to be 3.

The optimized method was tested on human leukocyte DNA. A sample (400 μg) was spiked with 1 pmol of each of the 18 standards, and a buffer blank (with no DNA) served as a negative control. The samples were enzymatically hydrolyzed and fractionated by HPLC. Twelve fractions were collected, dried, redissolved in H_2O, and analyzed. The negative control was similarly analyzed, and no trace of the adducts was detected. A reject mass list of 500 ions was used at a mass tolerance of ±5 ppm. This list consisted of the 2′-deoxyribonucleoside ions, their corresponding electrostatically bound dimer ions (reported in Table 1), and the most intense peaks observed in the sample preparation blank. The reject ion lists eliminate MS^2 fragmentation of ions, which are present in the background or due to the various processing steps. Figure 4 illustrates the power of the high-resolution/accurate mass detection used for this methodology. The observation of the triggered MS^3 spectrum corresponding to O^6-POB-dG in human leukocyte DNA allowed for the determination of the mass of the parent ion by examination of the full scan spectrum which immediately preceded the MS^3 event. Furthermore, the determination of the parent ion mass allowed for the generation of the extracted ion chromatogram from the full scan data. The ability to extract ions with 5 ppm mass tolerance allows for isolation of clear peaks (as shown in Panel C) from a high full scan background (shown in Panel A). In contrast, Panel B shows a chromatogram in which the peak is not clearly visible; this corresponds to the extracted ion signal under low-resolution/nominal mass accuracy (±0.2 amu) typical of ion trap and quadrupole instrumentation. Figure 5 summarizes the results obtained upon analysis of the 12 HPLC fractions. Clear peaks corresponding to 16 of the 18 adducts spiked into the DNA sample were detected in the accurate mass extracted ion chromatograms of the full scan data. More importantly, 14 of these adducts were identified by their corresponding MS^3 signal.

These promising results prompted us to test this analytical approach on samples from animals exposed to a DNA-adduct-inducing compound to verify its ability to detect and identify DNA adducts resulting from a specific exposure. 4-(Methylnitrosamino)-1-(3-pyridyl)-1-butanone (NNK), a potent rodent carcinogen, undergoes cytochrome-P450-mediated metabolism, resulting in the formation of species that react with DNA-forming adducts. Pyridyloxobutyl (POB)−DNA adducts and methyl−DNA adducts are among the major DNA modifications occurring after reaction of NNK metabolites with DNA. Among these adducts, O^6-POB-dG and O^2-POB-dT have been identified and quantified in liver and lung DNA of rats and mice

dx.doi.org/10.1021/ac403565m | Anal. Chem. 2014, 86, 1744−1752

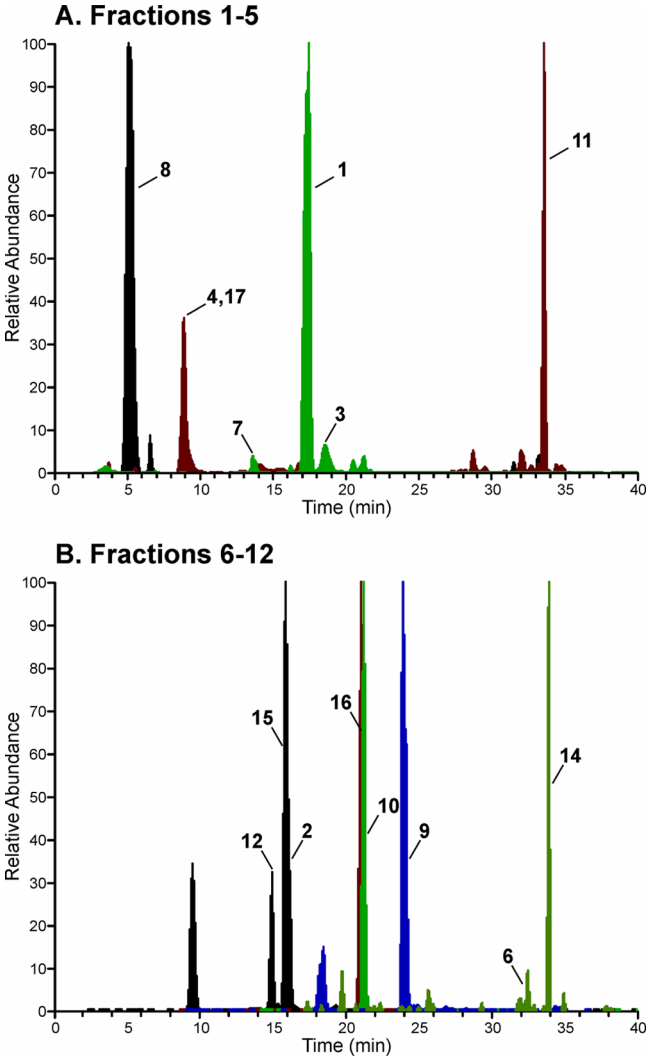

Figure 5. Extracted ion chromatograms (EIC) for standard mix adducts obtained upon analysis of the fractions obtained from the HPLC purification of a sample in which adducts were added to human leukocyte DNA. Numbers correspond to adduct identity (Figure 1). Panel A: superimposed EICs obtained from fractions 1−5. Panel B: superimposed EICs obtained from fraction 6−12. Each color refers to the single EIC.

exposed to NNK[18,20] in our laboratories, and therefore, [pyridine-D_4]O^2-POB-dT and [pyridine-D_4]O^6-POB-dG were available to be used as internal standards in our experiment. The two deuterated analogs (200 fmol each) were added to DNA isolated from liver of an A/J mouse exposed to NNK before hydrolysis. The sample was then hydrolyzed, and HPLC fractions were collected. To maximize sensitivity and identify adducts present at possibly very low levels, we made seven separate injections per fraction, analyzing for mass ranges of 50 amu to cover a total mass range of 250 to 600 amu. Multiple injections increased the required instrumentation time for each fraction but resulted in a significant increase in the sensitivity of the analysis. Triggered MS^3 signals corresponding to O^2-POB-dT and O^6-POB-dG and corresponding to the deuterated internal standards were detected in fractions 8 and 9, respectively. The full scan measured ion masses (390.1653 and 415.1716, respectively) which triggered the MS^2 and subsequently the MS^3 events had masses within 5 ppm (−1.6 ppm and +2.0 ppm, respectively) of the true masses (390.1660 and 415.1724, respectively). In addition, the MS^3 spectra closely matched spectra obtained from the synthetic standards. The observation of the internal standards (200 fmol) in this DNA sample (500 μg or 1.4 μmoles of bases) gives us a measure of the upper limit of the sensitivity of this methodology of ≤1.4 adducts per 10^7 nucleosides.

Additional DNA adducts identified in this experiment through examination of the MS^3 events were O^6-Me-dG in fraction 5, OH-PdG in fraction 6, and O^6-PHB-dG in fraction 9. O^6-Me-dG and O^6-PHB-dG are formed from NNK, whereas OH-PdG is an endogenous DNA adduct.[22] Figure 6 summarizes the MS^3 signals and chromatograms corresponding to the parent ions in the full scan event which triggered those MS^3 events.

This experiment confirmed the power of our "top down" methodology to reveal the presence of both unexpected and anticipated DNA adducts in in vivo samples through the combination of the full scan, MS^2, and MS^3 signals. Conventional DNA adduct discovery utilizes a "bottom up" approach where the formation of specific DNA adducts is hypothesized by considering the biochemistry of cytotoxins or suspected cytotoxins with confirmation by in vitro experimentation. This targeted approach, while more direct and technically more straightforward, does not account for the complexity of in vivo DNA adduct formation resulting from endogenous sources, such as oxidative stress or lipid peroxidation or as a result of exposure to complex mixtures of chemicals which cannot be completely anticipated or predicted. The high-resolution/accurate mass MS^n DNA adductomic approach outlined here requires no assumptions to be made, and the analysis, while technically challenging, can be performed directly on in vivo samples.

There are at least three significant advantages of using high-resolution/accurate mass monitoring for adductomics analysis. The accurate mass criterion for the observation of the neutral loss of the 2′-deoxyribose (116.0474 amu) provides a dramatic increase in the specificity of the adduct identification. Second, the accurate mass of an identified DNA adduct allows determination of its possible elemental composition. Third, our approach involves acquisition of MS^3 spectra which provide important structural information, including possibly the identity of the modified base. Triple-quadrupole-based adductomics approaches have been reported,[5−14] but they neither allow for accurate mass determination nor provide MS^3 spectra. In addition, the required scanning of quadrupoles limits the duty cycle of adduct detection and therefore the sensitivity of this approach relative to SIM or SRM analyses. We are not aware of any published examples of high-resolution/accurate mass adductomics approaches. Van den Driessche and co-workers[15] used Q-TOF instrumentation, but they did not report accurate mass measurements and also were limited to MS and MS^2 analysis. Turesky and co-workers[4] developed an adductomics approach similar to that reported here by utilizing triggering of MS^3 fragmentation upon observation of the neutral loss of 2′-deoxyribose. However, they used an ion trap instrument which limited the neutral loss triggering criteria to 116 ± 0.5 amu, not allowing for the high specificity of accurate mass measurement. In contrast, our method is based on the detection of adducts with a criteria of 116.0474 ± 0.0006 amu and determines the accurate molecular mass of both the parent and the fragment ions of the detected adducts. Additional innovations of the method presented here include lower flow (300 μL/min) for enhanced sensitivity, incorporation of background and artifact

dx.doi.org/10.1021/ac403565m | Anal. Chem. 2014, 86, 1744−1752

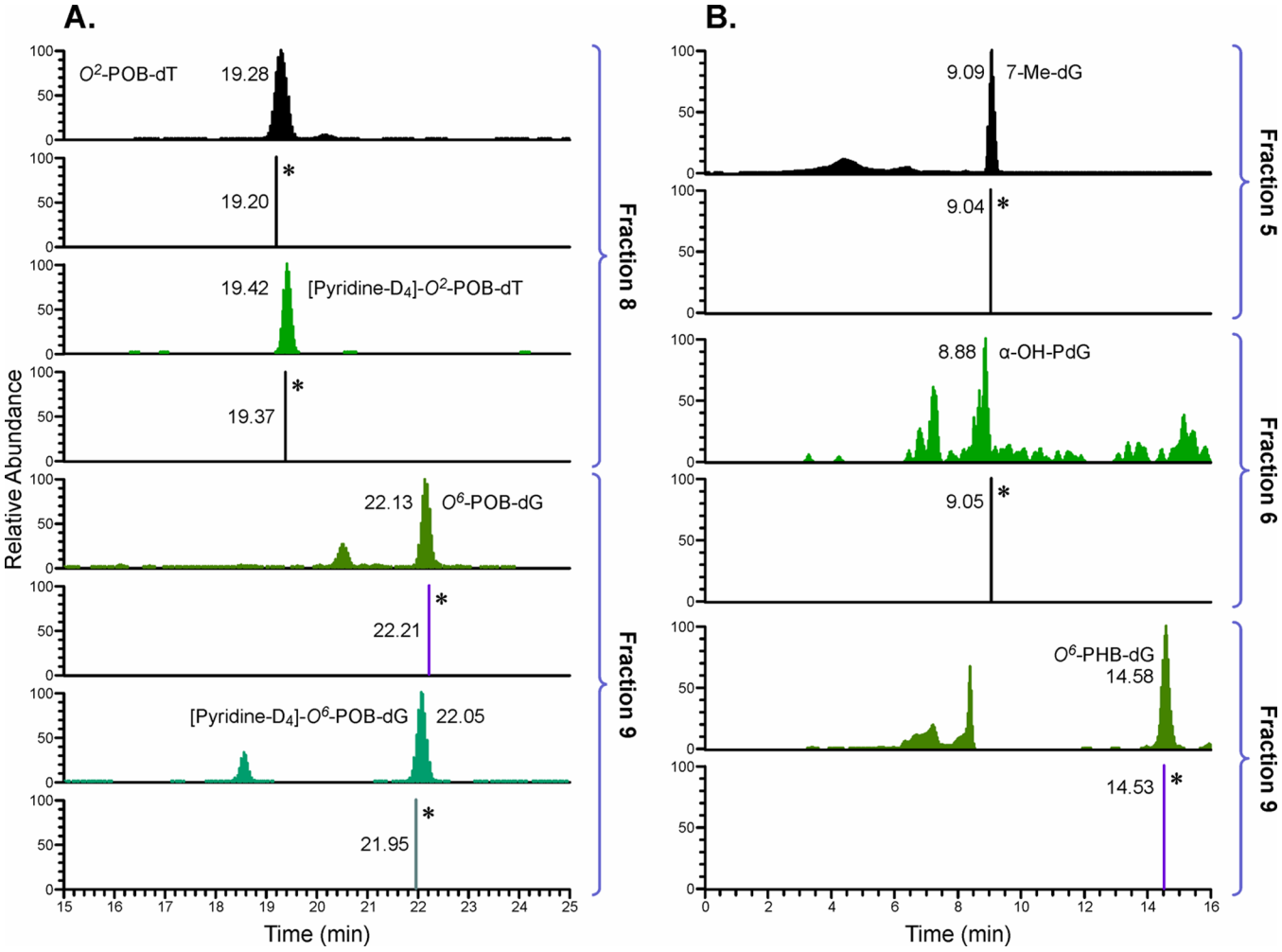

Figure 6. Chromatograms obtained upon analysis of liver DNA from mice exposed to NNK. The figure shows the chromatograms of the adduct detected in the full scan by the MS^3 signal (*) corresponding to the loss of 116.0474 amu. Panel A: POB adducts and their corresponding internal standards added before the DNA hydrolysis. Panel B: additional adducts detected in fractions 5, 6, and 9.

exclusion lists, and preanalysis fractionation for improved sensitivity.

The data reported here confirm the strength and potential power of our approach, but several areas of improvement are needed. The major issue limiting the sensitivity and ease of use of this method is the chemical complexity of the sample. This complexity prompted use of recombinant DNase, extensive fractionation, and multiple injections per fraction to achieve sufficient sample purification and sensitivity for low level DNA adduct detection. In spite of these efforts, the injected samples still showed significant chemical noise, a problem which requires further attention. One possible approach to decreasing background is the exclusive use of recombinant enzymes to perform DNA hydrolysis. In addition, the cell lysis and tissue processing solutions used for the isolation of DNA should be examined for their contribution to excessive chemical noise, and the DNA isolation process could be modified by including additional DNA purification after isolation. Changes in chromatographic separation could also be investigated to deal with the chemical complexity. Further optimization of MS^3 fragmentation parameters to improve fragment ion levels and increase the likelihood of the production of the protonated nucleobases of the corresponding DNA adducts might be useful. The detection of the MS^3 signal using the Orbitrap detector rather than the ion trap could be investigated to determine whether the benefits of accurate mass detection outweigh any reduction in sensitivity. In addition, the possibility of using higher energy collision-induced dissociation (HCD) fragmentation for MS^2 and MS^3 to increase the number of fragment ions thus providing additional structural information could be investigated.

■ CONCLUSION

The new field of DNA adductomics is still developing and challenges remain; however, the high-resolution/accurate mass MS^n methodology described here represents an important advance in the investigation of DNA adduct structures in complex mixtures. This approach could be an extremely powerful tool in the investigation of the effects on DNA of complex human exposures.

■ AUTHOR INFORMATION

Corresponding Author

*E-mail: balbo006@umn.edu. Fax: (612) 624-3869. Tel.: (612) 624-4240.

Notes

The authors declare no competing financial interest.

■ ACKNOWLEDGMENTS

The authors would like to thank Dr. Turesky of the Masonic Cancer Center and Medicinal Chemistry Department of the University of Minnesota for providing valuable comments and advice during the manuscript preparation and Bob Carlson for editorial assistance. This work was funded in part by NIH grants P30 CA077598-11 (Cancer Center Support Grant) and S10 RR024618-01A1 (Shared Instrumentation Grant).

■ REFERENCES

(1) Farmer, P. B.; Singh, R. *Mutat. Res.* **2008**, *659*, 68−76.
(2) Tretyakova, N.; Villalta, P. W.; Kotapati, S. *Chem. Rev.* **2013**, *113*, 2395−2436.
(3) Rappaport, S. M.; Li, H.; Grigoryan, H.; Funk, W. E.; Williams, E. R. *Toxicol. Lett.* **2012**, *213*, 83−90.
(4) Bessette, E. E.; Goodenough, A. K.; Langouet, S.; Yasa, I.; Kozekov, I. D.; Spivack, S. D.; Turesky, R. J. *Anal. Chem.* **2009**, *81*, 809−819.
(5) Chou, P. H.; Kageyama, S.; Matsuda, S.; Kanemoto, K.; Sasada, Y.; Oka, M.; Shinmura, K.; Mori, H.; Kawai, K.; Kasai, H.; Sugimura, H.; Matsuda, T. *Chem. Res. Toxicol.* **2010**, *23*, 1442−1448.
(6) Compagnone, D.; Curini, R.; D'Ascenzo, G.; Del Carlo, M.; Montesano, C.; Napoletano, S.; Sergi, M. *Anal. Bioanal. Chem.* **2011**, *401*, 1983−1991.
(7) Gangl, E. T.; Turesky, R. J.; Vouros, P. *Chem. Res. Toxicol.* **1999**, *12*, 1019−1027.
(8) Rindgen, D.; Turesky, R. J.; Vouros, P. *Chem. Res. Toxicol.* **1995**, *8*, 1005−1013.
(9) Kanaly, R. A.; Hanaoka, T.; Sugimura, H.; Toda, H.; Matsui, S.; Matsuda, T. *Antioxid. Redox Signaling* **2006**, *8*, 993−1001.
(10) Kanaly, R. A.; Matsui, S.; Hanaoka, T.; Matsuda, T. *Mutat. Res.* **2007**, *625*, 83−93.
(11) Matsuda, T.; Tao, H.; Goto, M.; Yamada, H.; Suzuki, M.; Wu, Y.; Xiao, N.; He, Q.; Guo, W.; Cai, Z.; Kurabe, N.; Ishino, K.; Matsushima, Y.; Shinmura, K.; Konno, H.; Maekawa, M.; Wang, Y.; Sugimura, H. *Carcinogenesis* **2013**, *34*, 121−127.
(12) Kato, K.; Yamamura, E.; Kawanishi, M.; Yagi, T.; Matsuda, T.; Sugiyama, A.; Uno, Y. *Mutat. Res.* **2011**, *721*, 21−26.
(13) Singh, R.; Teichert, F.; Seidel, A.; Roach, J.; Cordell, R.; Cheng, M. K.; Frank, H.; Steward, W. P.; Manson, M. M.; Farmer, P. B. *Rapid Commun. Mass Spectrom.* **2010**, *24*, 2329−2340.
(14) Spilsberg, B.; Rundberget, T.; Johannessen, L. E.; Kristoffersen, A. B.; Holst-Jensen, A.; Berdal, K. G. *J. Agric. Food Chem.* **2010**, *58*, 6370−6375.
(15) Van den Driessche, B.; Van Dongen, W.; Lemiere, F.; Esmans, E. L. *Rapid Commun. Mass Spectrom.* **2004**, *18*, 2001−2007.
(16) Gallagher, R. T.; Balogh, M. P.; Davey, P.; Jackson, M. R.; Sinclair, I.; Southern, L. J. *Anal. Chem.* **2003**, *75*, 973−977.
(17) Smith, R. D.; Shen, Y.; Tang, K. *Acc. Chem. Res.* **2004**, *37*, 269−278.
(18) Wang, M.; Yu, N.; Chen, L.; Villalta, P. W.; Hochalter, J. B.; Hecht, S. S. *Chem. Res. Toxicol.* **2006**, *19*, 319−324.
(19) Sturla, S. J.; Scott, J.; Lao, Y.; Hecht, S. S.; Villalta, P. W. *Chem. Res. Toxicol.* **2005**, *18*, 1048−1055.
(20) Lao, Y.; Villalta, P. W.; Sturla, S. J.; Wang, M.; Hecht, S. S. *Chem. Res. Toxicol.* **2006**, *19*, 674−682.
(21) Upadhyaya, P.; Kalscheuer, S.; Hochalter, J. B.; Villalta, P. W.; Hecht, S. S. *Chem. Res. Toxicol.* **2008**, *21*, 1468−1476.
(22) Zhang, S.; Villalta, P. W.; Wang, M.; Hecht, S. S. *Chem. Res. Toxicol.* **2007**, *20*, 565−571.
(23) Hecht, S. S.; Spratt, T. E.; Trushin, N. *Carcinogenesis* **1997**, *18*, 1851−1854.
(24) Melikian, A. A.; Amin, S.; Hecht, S. S.; Hoffmann, D.; Pataki, J.; Harvey, R. G. *Cancer Res.* **1984**, *44*, 2524−2529.
(25) Balbo, S.; Hashibe, M.; Gundy, S.; Brennan, P.; Canova, C.; Simonato, L.; Merletti, F.; Richiardi, L.; Agudo, A.; Castellsague, X.; Znaor, A.; Talamini, R.; Bencko, V.; Holcatova, I.; Wang, M.; Hecht, S. S.; Boffetta, P. *Cancer Epidemiol., Biomarkers Prev.* **2008**, *17*, 3026−3032.

■ NOTE ADDED AFTER ASAP PUBLICATION

This paper published ASAP on January 21, 2014. A change was made in "DNA Isolation from Mouse Liver", of the Experimental Section, and the revised version was reposted to the Web on February 4, 2014.